X-695-76-139
PREPRINT

NASA TM X- 71152

TERRESTRIAL KILOMETRIC RADIATION: 2-EMISSION FROM THE MAGNETOSPHERIC CUSP AND DAYSIDE MAGNETOSHEATH

JOSEPH K. ALEXANDER
MICHAEL L. KAISER

JUNE 1976

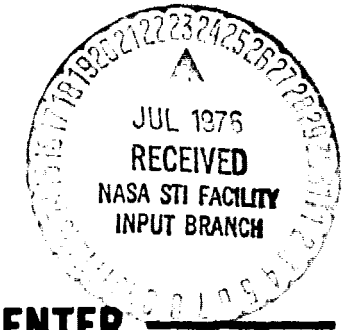

GSFC — GODDARD SPACE FLIGHT CENTER
GREENBELT, MARYLAND

TERRESTRIAL KILOMETRIC RADIATION: 2 - EMISSION FROM THE MAGNETOSPHERIC CUSP AND DAYSIDE MAGNETOSHEATH

Joseph K. Alexander and Michael L. Kaiser
Planetary Sciences Branch
Laboratory for Extraterrestrial Physics
NASA/Goddard Space Flight Center
Greenbelt, Maryland

ABSTRACT

Measurements of the location of sources of terrestrial kilometric radiation obtained with the lunar orbiting Radio-Astronomy-Explorer-2 satellite have revealed a class of emission associated with the cusp and dayside magnetosheath. At frequencies near 250 kHz this emission is observed at radial distances between 2 and 20 R_E at magnetic latitudes of 75^o to 80^o and is most often detected during periods of auroral activity (AE $\gtrsim$ 250) and southward orientation of the interplanetary magnetic field vertical component. During very disturbed times, the emission at the lowest frequencies ($\lesssim$ 200 kHz) appears to come from the dayside magnetosheath at distances $\gtrsim$ 12 R_E. Whenever the geomagnetic dipole is tilted significantly with respect to the ecliptic pole ($\gtrsim 10^o$) the cusp emission is confined to the hemisphere containing the sub-solar point. The measurements also suggest that the region of cusp emission is rather narrowly confined in longitude to within $\pm$ a few hours of the noon meridian.

I. INTRODUCTION

Recent satellite measurements of intense, nonthermal, kilometer wavelength radiation from the terrestrial magnetosphere suggest that this emission may amount to a significant fraction (perhaps as much as 1%) of the energy dissipated by the entire solar wind - magnetosphere interaction (Kennel, 1975). Although there is mounting indirect evidence that the terrestrial kilometric radiation (TKR) is a manifestation of magnetospheric substorms, our understanding of the role of the radio emissions must be preceded by the resolution of such basic properties as the physical location of the source. Studies by Gurnett and co-workers (Gurnett, 1974; Kurth et al., 1975) and by Kaiser and Stone (1975) showed that the most intense and most frequent TKR events were associated with the nighttime magnetosphere at auroral latitudes. A subsequent survey of the two-dimensional source position distribution as observed from lunar orbit (Kaiser and Alexander, 1975; Alexander and Kaiser, 1976) demonstrated that TKR could apparently originate from a wide range of locations and distances from the Earth and that a substantial portion of the emission is generated at high latitudes in the dayside hemisphere.

In this paper, we report on a more detailed study of the TKR sources in the dayside magnetosphere. This component of the emission appears to emanate from the polar cusp and adjacent regions in the dayside magnetosheath. Our objective is to provide an overview of the cusp emission which, when taken together with the results of correlative in situ measurements from other spacecraft, may eventually contribute to our understanding of the interaction of solar wind fields and particles with the terrestrial magnetosphere.

II. OBSERVATIONS

The technique for measuring two-dimensional source positions using RAE-2 lunar occultation observations was described in detail by Alexander and Kaiser (1976, hereinafter referred to as paper 1). Occultations of the Earth occur during every 222-min lunar orbit for a period of about one week every other week. Since the Earth is obscured from view by the lunar disk for $\sim$ 40 min during the occultation, the position determination derived from emission disappearance and reappearance times gives a "snapshot" of the source based on two brief "exposures" taken about 40 min apart in time. The source position is then displayed by projecting it onto the plane through the Earth at right angles to the Earth-Moon line. We attempt to deal with uncertainties in the occultation positions due to possible source motion or evolution during that $\sim$40 min interval by (1) requiring that the radio flux level be approximately the same at both the disappearance and reappearance ends of the occultation and (2) by looking at patterns in the source position distributions obtained from statistical compilation of a number of observations all obtained with the same viewing geometry in lunar phase. Repeatable patterns in such compilations demonstrate that there are clearly preferred regions of the magnetosphere from which the TKR is most often observed in spite of any uncertainties in the absolute location of individual sources (see paper 1).

The present study is based on the two-year survey of 250 kHz source locations described in paper 1. In order to insure that each

position determination was made at the frequency with greatest dynamic range, we re-analyzed each of these occultations at the frequency channel which showed the highest received power. This procedure resulted in a set of position measurements which are about equally distributed between observing channels at 210, 250 and 292 kHz. This frequency selection was influenced somewhat by instrumental effects since the RAE-2 receiver has slightly greater dynamic range and sensitivity below 300 kHz, the average frequency of peak TKR flux (paper 1). As we reported in paper 1, there is a tendency for the geocentric distance of TKR sources to increase with increasing wavelength, and hence, our selection of frequencies below the flux density peak will tend to slightly emphasize emission at large radial distances.

From the resultant set of occultations, we used only those observations that were obtained within $\pm$ 2.5 days of first quarter or last quarter moon so that RAE-2 was observing from a location within $\pm$ 3 hr of the dawn-dusk meridian plane. Consequently, the source positions derived from the lunar occultation events are projected on a plane that is approximately the noon-midnight meridian plane. From those observations, we have identified TKR sources that are unambiguously associated with the daytime hemisphere on 37 occasions between July 1973 and June 1975 representing about 15% of all TKR events observed during this time interval.

The occultation events with dayside emission used in the present study are listed in Table 1. The Universal Time for each event refers to the mid-point of the occultation; the actual immersion and emersion

times typically occur at $\pm$ 20 min of the U.T. listed. The geocentric radial distance given for each source can usually be determined with an rms uncertainty of $\pm$ 1 R_E. In some cases more than one radial distance is listed for an event because multiple emission components could be unambiguously identified. The invariant latitute, Λ, for each source was determined by projecting the occultation position onto the Mead and Fairfield (1975) MF73D model of the magnetospheric magnetic field in the noon-midnight meridian plane. The uncertainty in Λ of the source derived by this method decreases with increasing radial distance; for a source at the mean distance of 7 R_E it is about $\pm 3^{\circ}$. Also listed is the magnetic hemisphere (N = North, S = South) in which the source appears to be situated. The sixth and seventh columns in Table 1 pertain to the geometrical orientation of the Earth and Moon at the time of the observation. The local time (LT) at the sub-lunar point is given to indicate in what meridian plane RAE-2 was located when the position measurement was made. The tilt of the geomagnetic dipole is determined by the dipole latitude (absolute value) of the sub-solar point at the listed U.T. The last column lists the average value of the auroral electroject index (AE) for the 1-hr period centered on the midpoint of the occultation for all events for which AE data are presently available.

An example of a relatively simple occultation of a low-intensity source is shown in Figure 1 which gives the intensity-time plots at three frequencies (upper panel) and the source position geometry (lower panel) for the May 27, 1974, event. At all frequency channels

between 185 and 425 kHz this occultation gave essentially the same source position with a radial distance centered between 5 and 7 R_E and a projected invariant latitude of 75° to 76°.

Figure 2 is an example of a more complex (and more typical) occultation event observed on September 26, 1974. The primary component of the emission (A) leads to a source position at ~ 5 R_E geocentric distance and a projected invariant latitude of 78°. There is also evidence for a second, weaker component (B) at the lowest frequencies which would result in a source at R = 15 R_E in the magnetosheath.

In addition to those occultation events which show one or more source components that are clearly located in the dayside hemisphere within ~ 15 R_E of the Earth, there are a number of occultation events in which the emission region is apparently never completely occulted even though the entire magnetosphere is obscured by the lunar disk. These events, which occur most often at the lowest TKR frequencies, provide strong evidence for a component of the dayside emission that probably originates in the magnetosheath. Figure 3 is an example of such an event observed from above the dusk sector on December 4, 1973. At 250 kHz and at higher frequencies the most intense emission disappears and reappears at time that would place the source near the Earth. There is a weaker component to the 250 kHz emission that is apparently occulted only between 0934 and 0942, and this component must extend out to a distance of ~ 14 R_E. The situation is most dramatically illustrated at 185 kHz where the noise level remains

≥ 20 dB above the background throughout the entire occultation period! As the arrow in the lower panel of Figure 3 indicates, there must be a significant source of intense radiation at 185 kHz at a distance of greater than 13 R_E during this event.

In Table 2 we have listed the circumstances for the occultation events of the type illustrated in Figure 3 where there is unambiguous evidence for source locations at magnetosheath distances. The table lists events where the TKR intensity was ≥ 10 dB above background in at least one frequency channel between 185 and 292 kHz during the entire occultation period. The mid-time of the occultation period is given in the second column. Since these events are all incomplete occultations at the lowest TKR frequencies, the distances given in the third column are minimum distances to the source at frequencies less than or equal to the frequency listed in column four. Also given are the local time of the sub-lunar point and the tilt of the geomagnetic dipole at the time of the observation. The average value of the AE index for the 1-hr period centered on the occultation midpoint is listed in the last column. The monotonic decrease in minimum distance as a function of time on December 4, 1973, does not necessarily imply inward motion of the source but is most likely due to the changing geometry of the lunar occultations on that day.

III. RESULTS

As is illustrated in Figure 4, the dayside TKR sources listed in Table 1 are apparently confined to projected invariant latitudes between about 64° and 80°. The mean value of Λ for the 50 individual

source regions identified in the occultation data is 74° (6° standard deviation); however over 50% of the sources were observed at projected latitudes between 75° and 80°. There is evidence for a bimodal latitude distribution, but it may not be statistically significant in view of the uncertainty in estimating Λ. On the other hand, the sharp high-latitude cutoff at 80° is probably real. The source latitude distribution provides strong evidence that the dayside sources are associated with the magnetospheric cusp, and we shall discuss this point in more detail subsequently.

There is also evidence that the dayside emission is associated with the occurrence of magnetospheric substorms. As Figure 5 shows, the AE distribution for cusp emission events is markedly different from the AE distribution for all times during the 1973 observing period. Based on an analysis of the AE index for the first 20 of the 37 events in Table 1 (AE data are only available through March 1974 at this writing), we find that hourly averages of AE were greater than 250 γ for 50% of the dayside events and were below 150 γ on only four occasions. Furthermore, we find that the vertical component of the interplanetary magnetic field was directed Southward in 19 out of 28 events for which interplanetary magnetic field data were available. For the events with unocculted emission at large radial distances listed in Table 2, AE exceeded 250 γ in every case and had an average value of $\sim$ 400 γ.

The variation of radial distance and invariant latitude as a function of AE for the dayside sources is shown in Figure 6. Although there are no obviously strong correlations apparent in either distribution there is some evidence that the <u>maximum</u> radial distance at

which dayside source components can be observed is a function of AE. We observe emission at magnetosheath distances only when AE exceeds $\sim$ 200 γ. Extrapolation to times of very low AE would predict that the emission would be observed only at distances less than $\sim$ 2 R_E. Recent studies of the latitude dependence of the magnetospheric cusp as a function of substorm activity (Kamide et al., 1976) would suggest that we might observe the latitude of the cusp emission to decrease with increasing AE, but there is no statistically significant trend in that direction in Figure 6. This may not be too surprising since the average equatorward motion of the cusp during typical substorms is essentially equal to our measurement uncertainty in latitude.

The positions of all the sources listed in Table 1 are displayed in the superposed projections in Figure 7. Recall that since all the occultation measurements were obtained when RAE-2 was within $\pm$ 3 hr of the dawn-dusk meridian plane, the projection plane in Figure 7 is the noon-midnight meridian plane $\pm$ 3 hr. We have used the modified geocentric solar magnetic co-ordinate system described in paper 1 in which the Z axis contains the projection of the geomagnetic dipole axis, the +Z hemisphere contains the daytime magnetic pole, and the sun is in the +X hemisphere. The source position compilations have been sorted according to the tilt of the geomagnetic dipole.

The most remarkable feature of Figure 7 is the way the scatter in the source locations changeswith dipole tilt angle. For events with low tilt ($\leq 10^{\circ}$) the sources appear to be distributed over a wide range in latitude as well as distance. For events with intermediate

($10^\circ < \text{tilt} < 22^\circ$) and high ($\geq 22^\circ$) tilt angles, however, the emission appears to originate almost exclusively from the +Z hemisphere near the latitude of the polar cusp. There is also some evidence that the source latitude tends to decrease with decreasing radial distance. This effect is probably the result of refraction of the radio waves in the outer plasmasphere since sources at low altitudes will appear to be shifted equatorward if significant refraction occurs along the ray path through the plasmasphere.

Aside from the strong hemispherical asymmetry due to the sources being situated in the magnetic hemisphere associated with the daytime pole and the small dispersion in latitude for events with high tilt, there are no other obvious patterns in the position distribution. As we noted in paper 1, emission at larger distances is generally weaker and confined to lower frequencies than emission at low altitudes. We also tend to observe the cusp emission more often when RAE-2 is situated over the dusk side of the Earth rather than over the dawn side, but the source location statistics seem to remain the same for either viewing geometry.

IV. DISCUSSION

To facilitate our discussion of the implications of the dayside TKR measurements we will first recapitulate the key points of the preceding section. The principal observational properties of the emission may be summarized as follows:

1) dayside sources are concentrated at "auroral" latitudes (74° - 80°) and have a sharp high-latitude cutoff at $\Lambda \simeq 80^\circ$;

2) emission is observed to originate from geocentric radial distances ranging from $\lesssim 2$ to > 15 R_E;

3) dayside TKR events are most often associated with periods of enhanced AE ($\gtrsim 250$ γ) and Southward B_z; and

4) during times of significant dipole tilt with respect to the ecliptic pole, the emission is associated only with that magnetic hemisphere that includes the sunlit magnetic pole.

As we have already noted, the latitude distribution of the dayside TKR sources argues strongly that they are associated with the polar magnetospheric cusp. Furthermore, those occultation events which show emission far from the Earth at magnetosheath distances are all consistent with a source location in the region of the cusp-magnetosheath interface. The 80° cutoff in the latitude distribution provides evidence that the longitude or local time extent of the cusp emission region is rather narrow. In our survey, any sources at cusp latitudes that were located significantly out of the noon meridian plane, would appear to be at latitudes greater than 80° when shown projected onto the noon-midnight meridian plane. Since we see no evidnece for such foreshortening effects, we can estimate that the local time extent may not exceed $\sim \pm 2$ hr.

The occurrence of cusp emission preferably in the magnetic hemisphere that includes the daytime pole may be important evidence that the dayside emission is a consequence of the processes of entry of particles into the magnetosphere from the solar wind. For example, if magnetic field line merging occurs near the vicinity of the subsolar

point in the magnetosphere when the interplanetary field is Southward, then particles which enter (and are possibly accelerated) there will flow back toward the cusp. When the dipole tilt angle is large, those particles on field lines originally connected to the merging region may have more direct access to the cusp in the +Z hemisphere due perhaps to the closer proximity of the subsolar point to the +Z cusp or to a more favorable magnetic field geometry in that hemisphere.

There have been a number of important in situ observations of waves in the vicinity of the polar cusp prior to the remote survey by RAE-2, and it is appropriate to consider the dayside TKR as one element of a complex ensemble of wave phenomena which can be observed in that region of the magnetosphere. Using OGO-5 plasma wave data at ULF and VLF frequencies, Scarf and co-workers observed intense wave levels during a major geomagnetic storm both in the low altitude cusp (Scarf et al., 1972) and in the interface region between the cusp and the magnetosheath (Scarf et al., 1974). In summarizing subsequent work to interpret the OGO-5 observations, Fredericks (1975) discussed the implications of the cusp wave measurements in terms of field-line merging near the subsolar point as an energy source for field-aligned currents in the cusp that could flow into the dayside auroral ionosphere. Measurements at VLF and MF frequencies on OGO-4 (Laaspere and Hoffman, 1974) and ISIS-2 (Hartz and James, 1974) have also shown that a variety of emissions at frequencies up to ~0.5 MHz can be observed in the polar cusp. Although good progress has been made in accounting theoretically for the origin of the VLF emissions, the physical relationship between

the waves observed in situ and the high frequency TKR emissions observed remotely is not yet clear. The problem is a compelling one, however, because the rich collection of wave phenomena in the dayside magnetosphere should provide effective diagnostic signatures for physical processes that are important not only in the terrestrial magnetosphere but in many astrophysical plasmas.

ACKNOWLEDGEMENTS

We are grateful to Ms. P. Harper and S. Vaughan for their assistance with the data analysis and to our colleagues R. F. Benson, D. H. Fairfield, N. F. Ness and R. G. Stone for helpful discussions. Auroral electrojet index (AE) data used in connection with this article were obtained from World Data Center - A for Solar-Terrestrial Physics (Geomagnetism).

REFERENCES

Alexander, J.K. and M.L. Kaiser, Terrestrial kilometric radiation: 1-Spatial structure studies, submitted to J. Geophys. Res. (also GSFC Rept. X-693-76-47), 1976.

Fredricks, R.W., Wave particle interactions in the outer magnetosphere: A review, The Magnetospheres of the Earth and Jupiter, V. Formisano ed., p. 113, D. Reidel, Dordrecht, Holland, 1975.

Gurnett, D.A., The Earth as a radio source: Terrestrial kilometric radiation, J. Geophys. Res., 79, 4227, 1974.

Hartz, T.R., and H.G. James, The distribution of ionospheric M.F. noise emission relative to the cleft, EOS Trans. AGU, 55, 70, 1974.

Kaiser, M. L., and R.G. Stone, Earth as an intense planetary radio source: Similarities to Jupiter and Saturn, Science, 189, 285, 1975.

Kaiser, M.L. and J.K. Alexander, Source location measurements of terrestrial kilometric radiation obtained from lunar orbit, Geophys. Res. Lett., 3, 37, 1976.

Kamide, Y., J.L. Burch, J.D. Winningham, and S. -I. Akasofu, Dependence of the latitude of the cleft on the interplanetary magnetic field and substorm activity, J. Geophys. Res., 81, 698, 1976.

Kennel, C.F., What we have learned from the magnetosphere, Comments Astrophys. Space Phys., 6, 71, 1975.

Kurth, W.S., M.M. Baumback and D.A. Gurnett, Direction-finding measurements of auroral kilometric radiation, J. Geophys. Res., 80, 2764, 1975.

Laaspere, T., and R.A. Hoffman, Observations of the correlation between cleft-region electrons and VLF auroral hiss, EOS Trans. AGU, 55, 71, 1974.

Scarf, F.L., R.W. Fredricks, I.M. Green, and C.T. Russell, Plasma waves in the dayside polar cusp, 1, magnetospheric observations, J. Geophys. Res., 77, 2274, 1972.

Scarf, F.L., R.W. Fredricks, M. Neugebauer, and C.T. Russell, Plasma waves in the dayside polar cusp, 2, magnetopause and polar magnetosheath, J. Geophys. Res., 79, 511, 1974.

Table 1. RAE-2 Magnetospheric Cusp Emission Observations

Date	U.T.	R/R_E	Λ	Hem.	LT	Tilt	AE
1973							
Sept. 23	0050	3.0	67°	S	8.9 hr	6°	438
Oct. 19	1259	4.7,5.6	69,67	N,S	6.5	3	400
20	0351	2.6	65	S	7.0	21	509
Nov. 5	2120	15.2	77	S	19.7	11	272
6	0442	4.4	75	S	20.1	27	79
6	1208	9.7	77	S	20.3	11	147
6	1933	5.2,10.6	76,78	S	20.5	7	474
6	2317	2.7	68	S	20.6	14	280
15	0836	3.3	64	S	4.3	23	260
15	1215	6.9	75	S	4.5	13	188
15	1943	2.5	66	S	4.8	10	199
16	0652	5.0,12.2	75,79	S	5.1	27	210
Dec. 3	2235	3.3	67	N	18.5	20	289
4	1323	2.2,5.8,9.8	80,76,77	S	19.0	14	425
13	0951	7.0	78	S	3.2	25	145
13	1714	4.5	68	S	3.4	11	94
30	0313	9.0,16.0	80,79	S	15.8	34	222
31	0853	2.1	65	N	17.2	27	249
31	1618	2.7	73	S	17.1	11	283
1974							
Mar. 3	0908	4.0	71	S	19.5	11	178
Apr. 30	1144	4.1	72	N	19.2	17	
30	2252	5.2	72	N	19.6	14	
May 27	0719	5.1	76	N	17.1	11	
June 10	0951	8.4	80	N	4.1	19	
Sept. 23	0505	15.3	77	S	17.8	11	
25	1624	8.7	78	S	19.7	10	
25	2008	5.2	77	S	19.8	6	
26	1058	5.7	78	S	20.3	0	
26	1440	9.2	73	S	20.4	8	
26	1821	6.6,14.7	83,77	S	20.5	8	
Oct. 7	1500	4.3	63	S	4.8	5	
22	0815	12.5,16.8,21.2	78,78,78	S	17.4	17	
23	0632	2.8	90	S	18.1	21	
1975							
Mar. 3	1328	3.2	66	N	4.9	1	
6	1154	4.8	64	N	7.4	1	
21	0127	3.0,16.8	64,77	N	18.3	7	
May 14	2255	2.8,6.4,8.4,11.2	64,68,74,78	N	15.1	18	

Table 2. Incomplete Occultation Events

Date	U.T.	Min. R/R_E	Frequency	LT	Tilt	AE
1973						
Nov. 7	0259	16	250 kHz	21.0 hr	25°	284
7	0640	14	185	21.1	26	330
Dec. 4	0214	18	210	18.8	31	284
4	0939	14	250	19.0	25	582
4	1323	12	210	19.1	14	425
4	1704	10	210	19.3	10	739
1974						
Sep. 25	2350	25	210	19.9	3	
26	1440	18	250	20.2	8	
26	1821	16	250	20.3	8	

Fig. Captions

Fig. 1. Example of an occultation of a source of kilometer wavelength emissio from the dayside hemisphere. The upper panels are intensity vs. time displays for the 1-hr period centered on the occultation mid-time. The lower panel shows the source location projected on the plane perpendicular to the Earth-Moon line. The disappearance and reappearance times denoted by the hatched bars in the upper panel result in a source position given by the cross-hatched area in the lower panel. In the lower panel, the dashed lines show the projected position of the lunar limb at 2-min intervals and the solid lines show magnetospheric magnetic field lines near the polar cusp as given by the Mead-Fairfield MF73D magnetic field model.

Fig. 2. Example of a typically complex occultation event of dayside emission displayed in the same format as Figure 1. The most intense source (A) disappears at time A_1 and reappears at time A_2. At frequencies near 200 kHz, a second, weaker component (B) is apparently occulted between times B_1 and B_2. In the lower panel the lunar limb positions are projected at 5-min intervals (dashed lines), and nominal magnetospheric cusp and bow shock locations are shown (solid lines) for reference.

Fig. 3. Example of an occultation event in which the source region at frequencies below 250 kHz is apparently never completely obscured. The dashed lines in the upper panels show the background levels to which the signal level would fall during a complete occultation event. The arrow in the lower panel shows the limit to the source location (minimum distance) required at frequencies $\lesssim$ 200 kHz. The magnetospheric magnetic field lines are again from the Mead-Fairfield MF73D model and are shown along with a nominal bow shock for reference.

Fig. 4. Invariant latitude distribution (in 3° increments) of the dayside sources listed in Table 1 derived from projection onto the Mead-Fairfield MF73D model in the noon-midnight meridian plane.

Fig. 5. Distribution of 1-hr averages of the auroral electrojet index (AE) for dayside emission occultation events (lower histogram) compared with the AE occurrence distribution for all times during 1973 (upper histogram). The gap in the occurrence of cusp events for $300 < AE < 400$ is presumably due to the small statistical sample.

Fig. 6. Variation of AE (1-hr average) for the times of dayside TKR occultation events as a function of projected geocentric radial distance to the source (upper plot) and projected invariant latitude (lower plot). The open circles in the upper diagram denote the minimum distances for the incomplete occultations listed in Table 2. The dashed line in the radial distance plot indicates a possible variation of maximum distance as a function of AE.

Fig. 7. Projections of the dayside TKR source locations onto the Mead-Fairfield MF73D magnetospheric magnetic field model in the noon-midnight meridian plane. The data are sorted according whether the tilt of the geomagnetic dipole with respect to the ecliptic pole was low (tilt $\leq 10^{\circ}$), medium ($10^{\circ} < \text{tilt} < 22^{\circ}$), or high (tilt $\geq 22^{\circ}$).

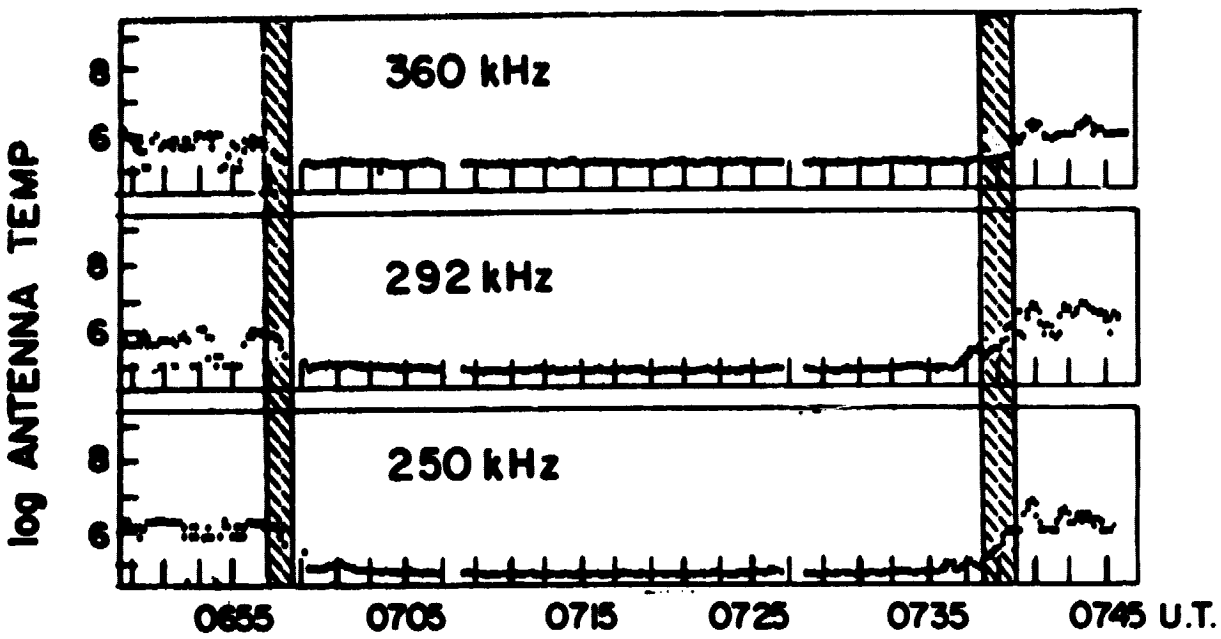
log ANTENNA TEMP
8
6
360 kHz
292 kHz
250 kHz
0655
0705
0715
0725
0735
0745 U.T.

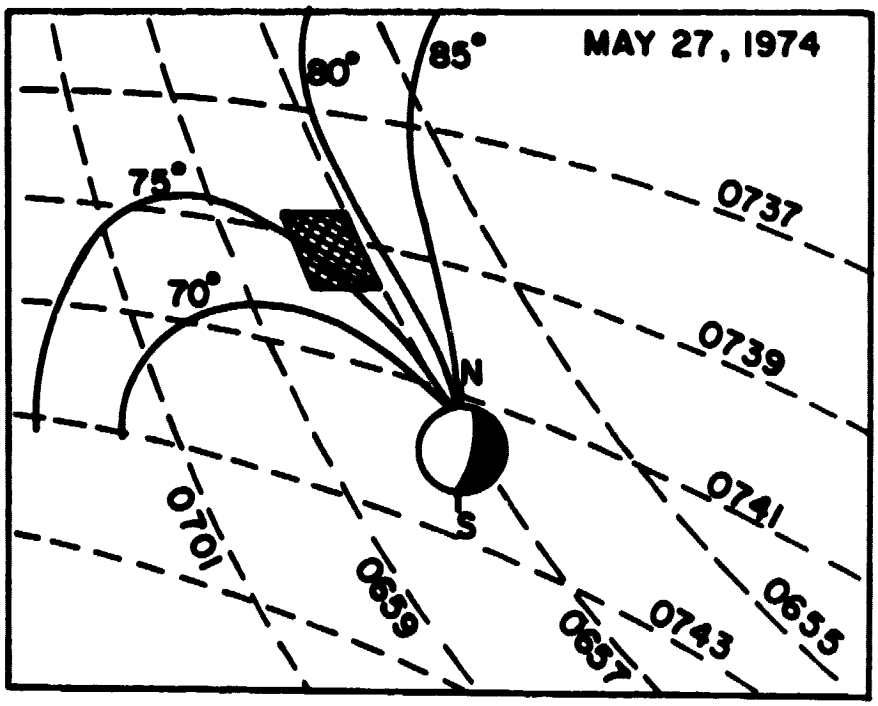
MAY 27, 1974
90°
85°
75°
70°
0737
0739
0741
0743
0655
0657
0659
0701
N
S

Fig. 1

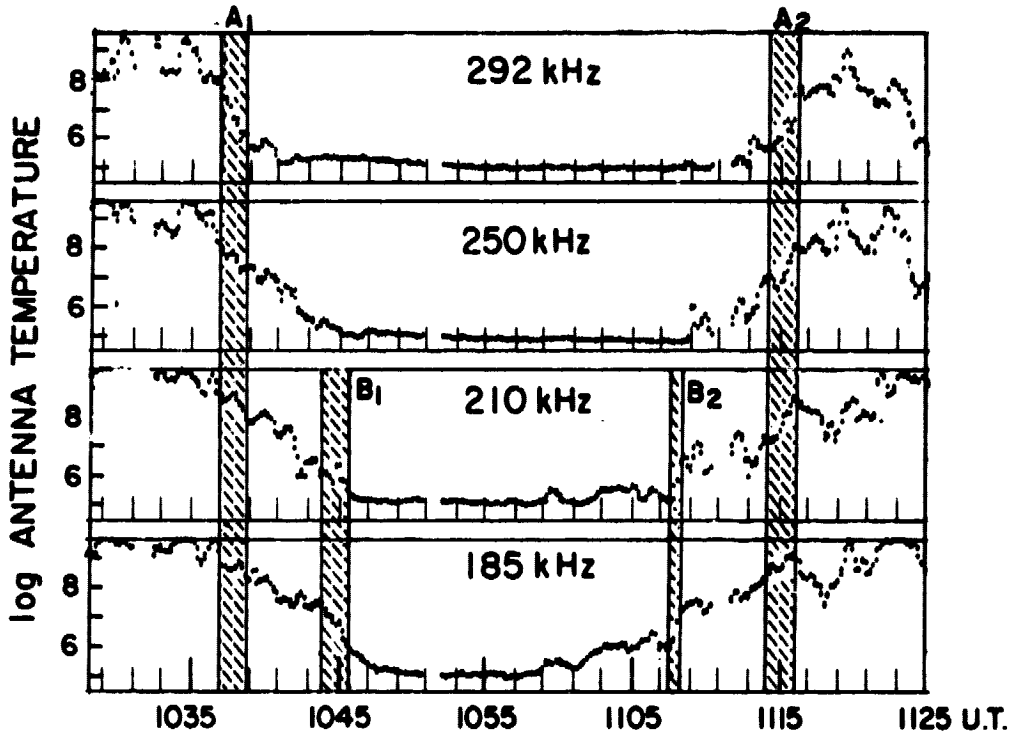
A1
A2
292 kHz
250 kHz
B1
210 kHz
B2
185 kHz
log ANTENNA TEMPERATURE
8
6
1035
1045
1055
1105
1115
1125 U.T.

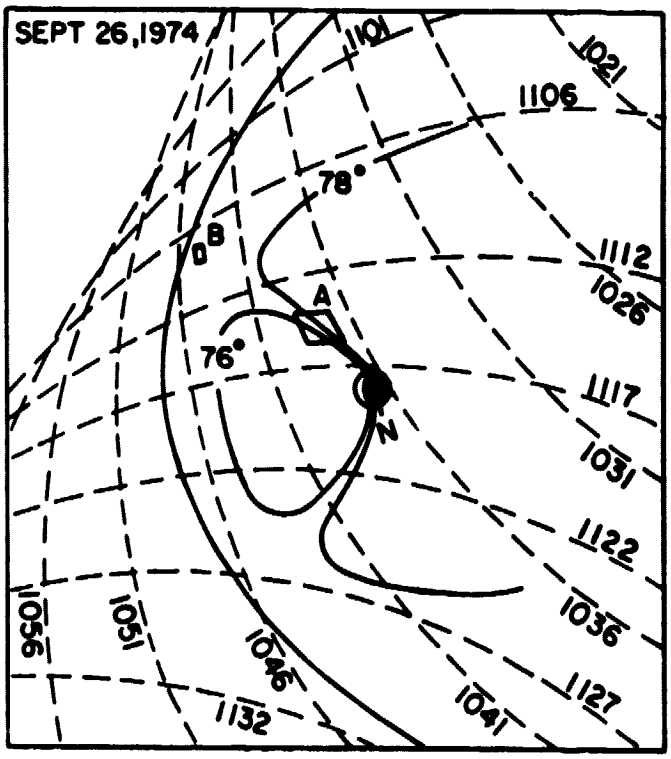
SEPT 26,1974
1101
1021
1106
78°
B
A
1112
1026
76°
1117
1031
1122
1036
1127
1041
1046
1051
1056
1132

FIG. 2

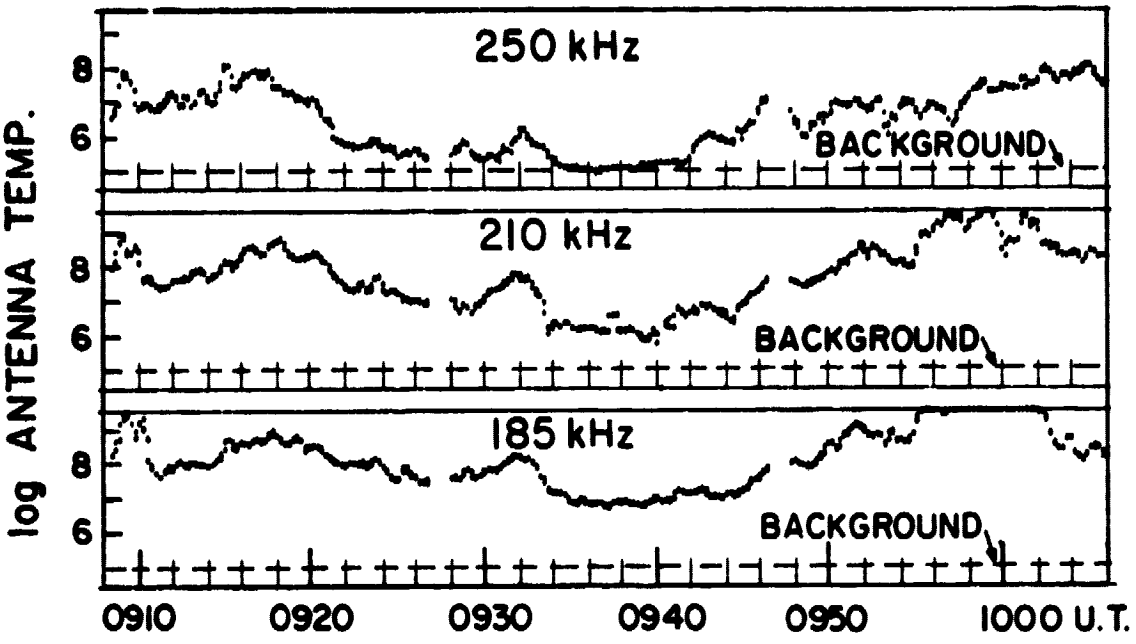
250 kHz
BACKGROUND
210 kHz
BACKGROUND
185 kHz
BACKGROUND
log ANTENNA TEMP.
8
6
0910
0920
0930
0940
0950
1000 U.T.

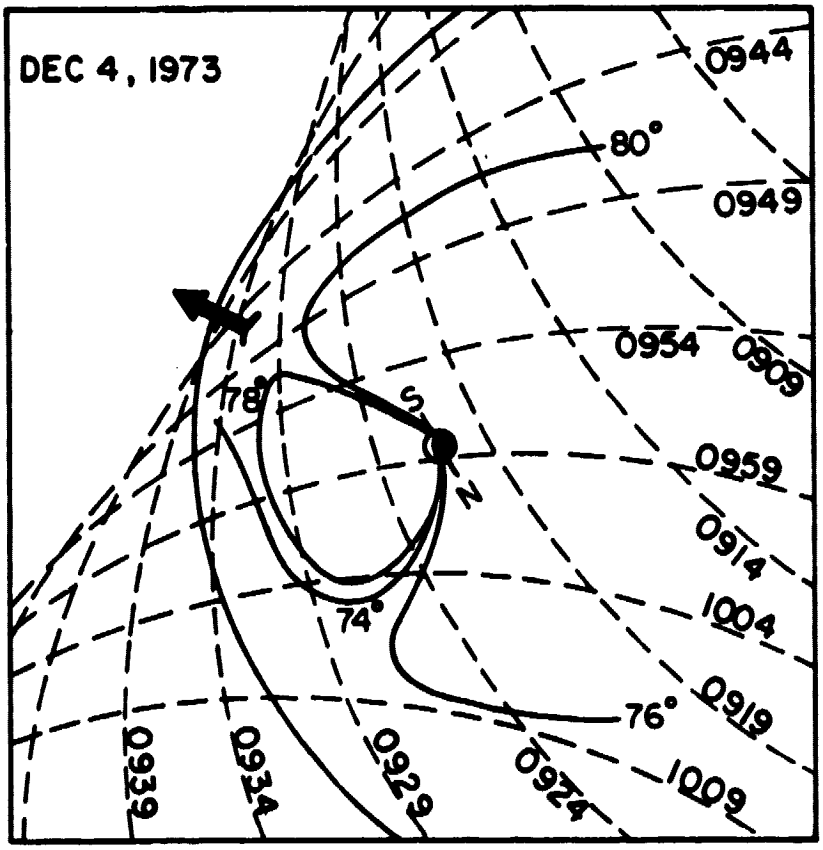
DEC 4, 1973
0944
80°
0949
0954
0909
78°
S
0959
N
0914
74°
1004
0919
76°
1009
0939
0934
0929
0924

FIG. 3

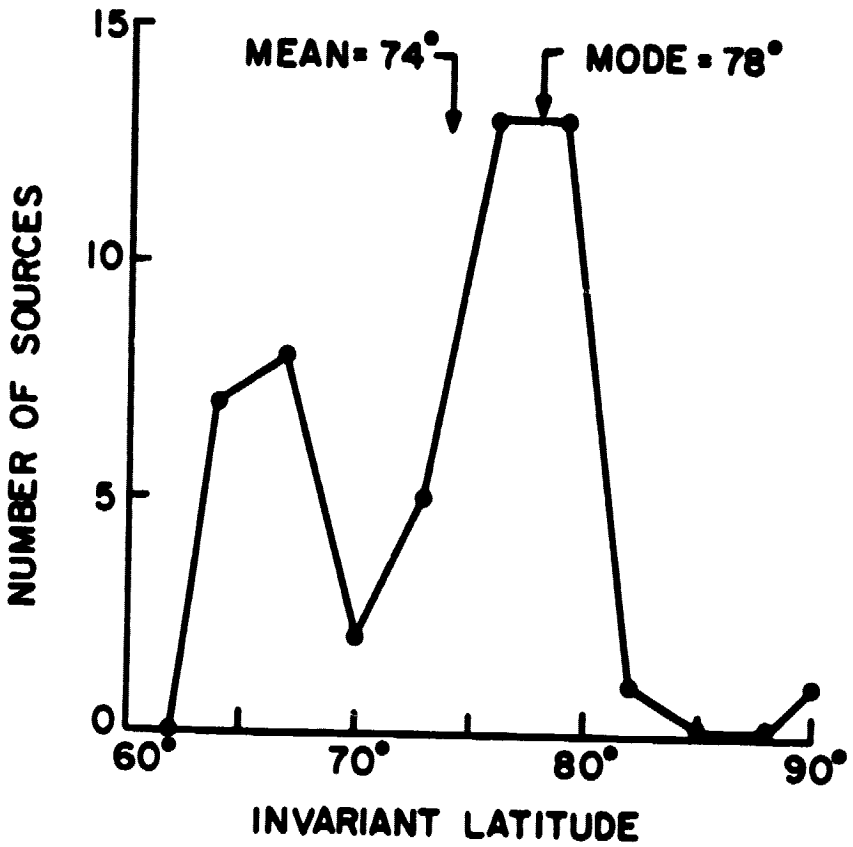
MEAN= 74°
MODE = 78°
15
10
5
0
NUMBER OF SOURCES
60°
70°
80°
90°
INVARIANT LATITUDE

FIG. 4

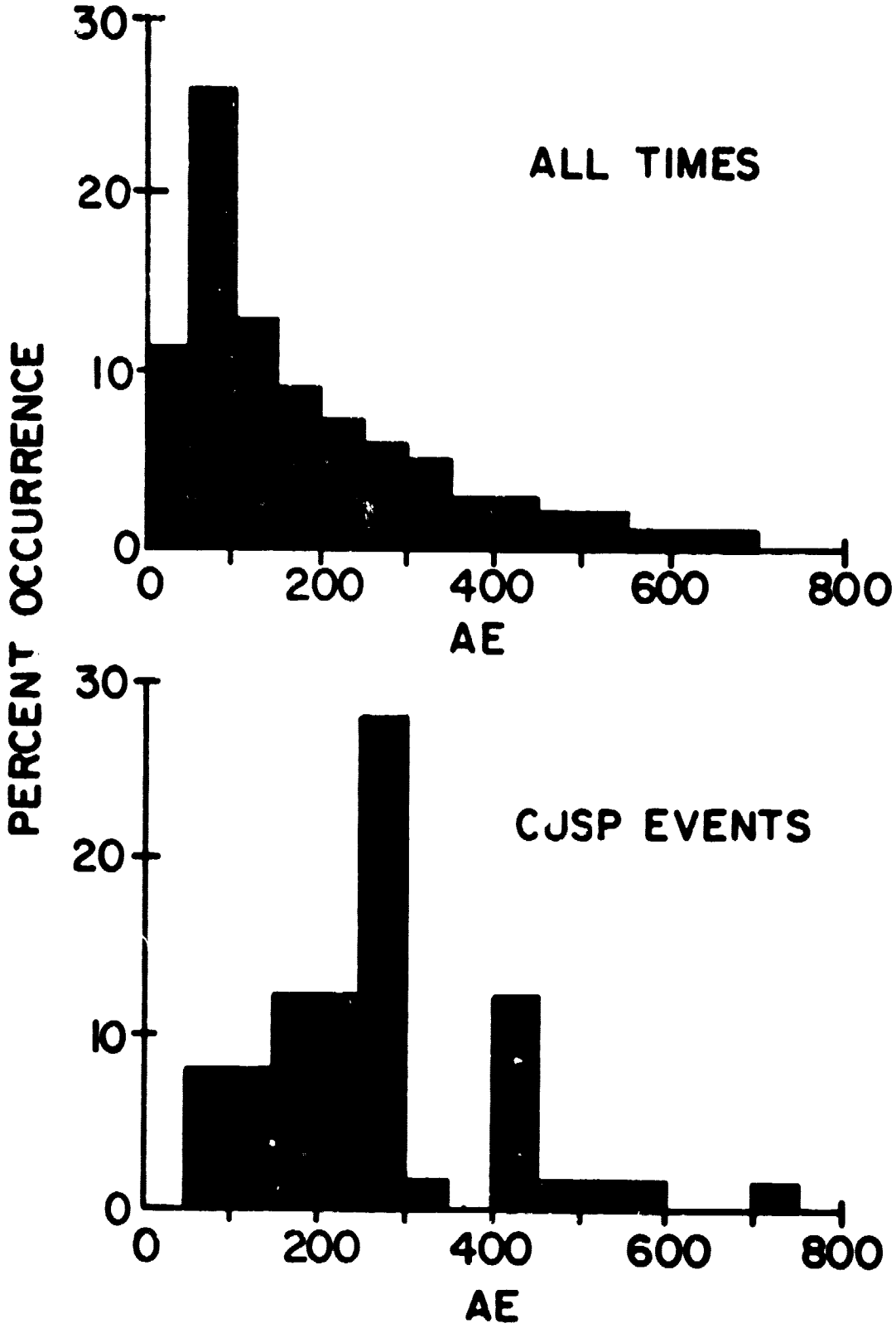
30
20
10
0
PERCENT OCCURRENCE
ALL TIMES
0
200
400
600
800
AE
30
20
10
0
CUSP EVENTS
0
200
400
600
800
AE

FIG. 5

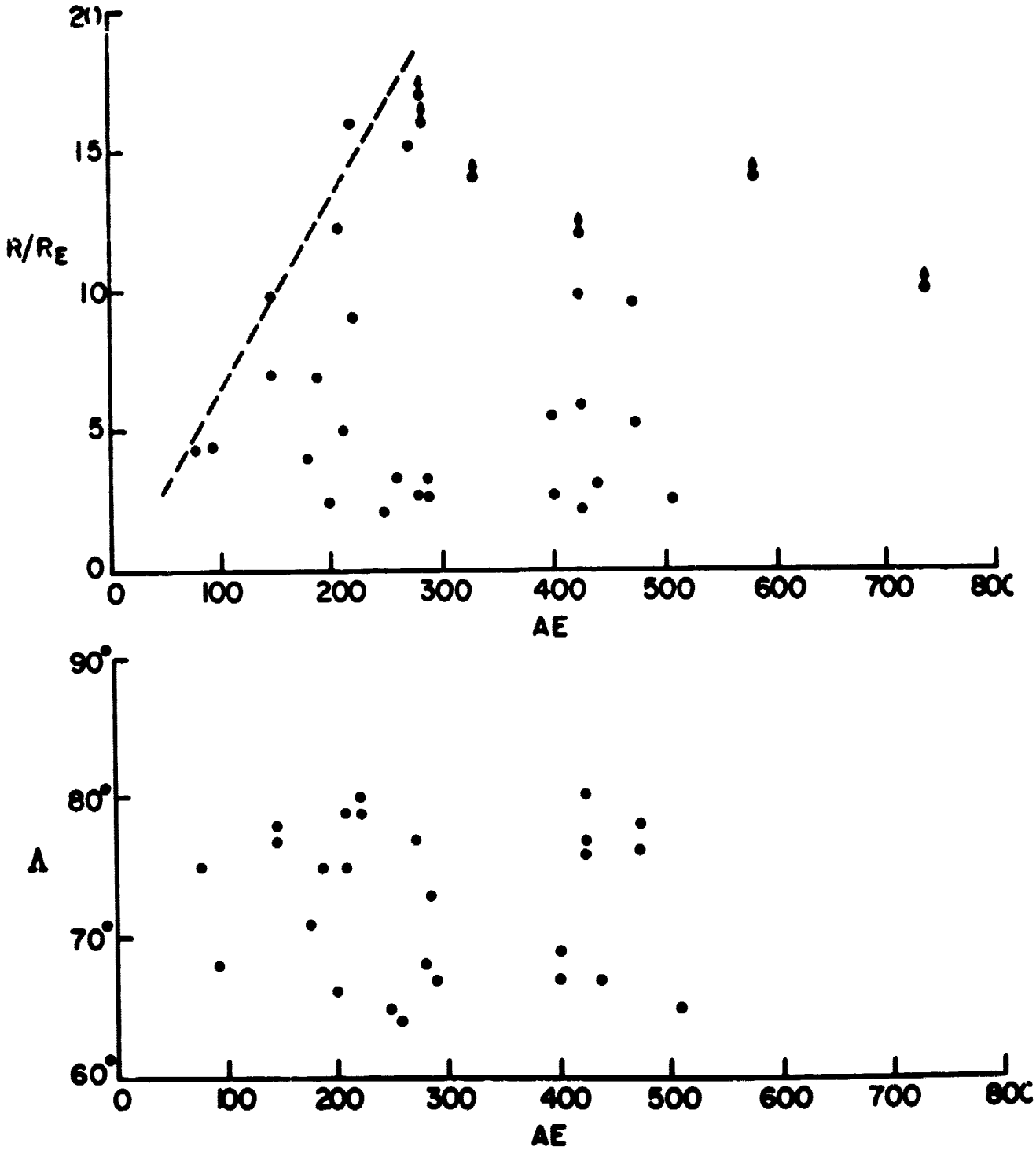
20
15
10
5
0
R/R_E
0
100
200
300
400
500
600
700
800
AE
90°
80°
70°
60°
Λ
0
100
200
300
400
500
600
700
800
AE

FIG. 6

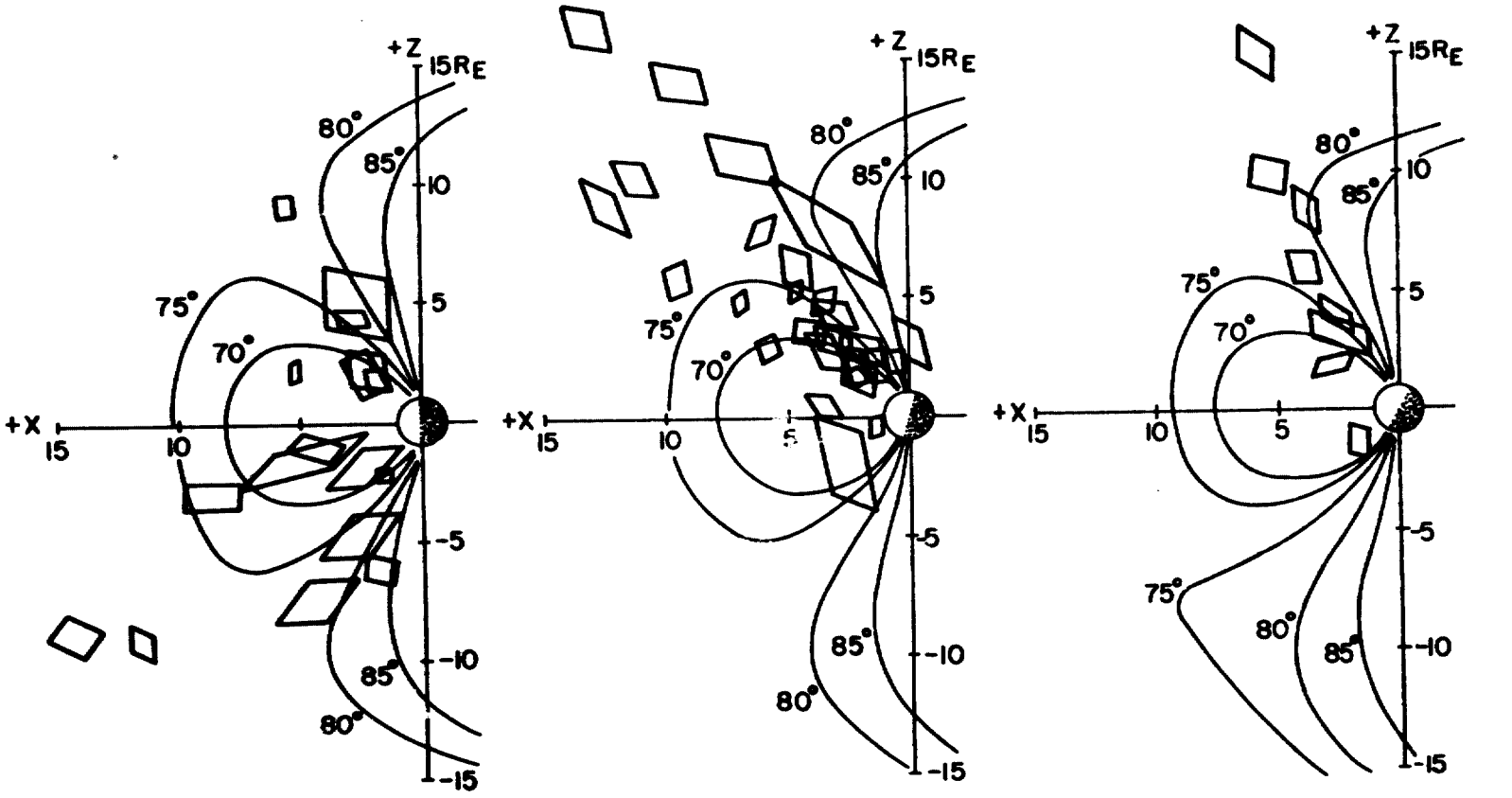
+Z
15R_E
80°
85°
10
5
75°
70°
+X
15
10
-5
-10
-15
(a) MINIMUM TILT
(b) INTERMEDIATE TILT
(c) MAXIMUM TILT

FIG. 7